

# One-touch friction estimation at the onset of grasp

Giuseppe Vitrani  
Cognitive Robotics Department  
Delft University of Technology  
g.vitrani@tudelft.nl

Laurence Willemet  
Cognitive Robotics Department  
Delft University of Technology  
l.willemet@tudelft.nl

Michaël Wiertelwski  
Cognitive Robotics Department  
Delft University of Technology  
m.wiertelwski@tudelft.nl

**Abstract**—Safe robotic grasping requires knowledge of surface friction before any lift attempt. Current approaches either rely on dangerous slip events or are confined to flat surfaces. Here, we present a method that classifies surface slipperiness from a single normal press using high-resolution tactile sensing. A supervised autoencoder maps the normalized lateral displacement magnitude field into a one-dimensional latent space where friction regimes separate linearly, independently of contact geometry. The method was validated using the seven indenter geometries considered during acquisition and tested on unseen objects under both dry and lubricated conditions. The model achieves consistent pre-lift friction identification, enabling proactive grasp adjustment.

## INTRODUCTION

Routine manipulation tasks like lifting a wet glass or grasping a delicate fruit require the hand to continuously regulate contact forces against the risk of slip. This regulation critically depends on an estimate of friction at each contact point. When friction is overestimated, the planned grasp may fail upon lift because the cone of friction is narrower than assumed, making force closure unachievable in practice [1]. Despite this dependence, most grasp planners treat friction as a fixed prior rather than a measurable quantity [2].

Tactile sensors give access to contact interactions, unlocking friction information for the robotic manipulator. A common approach detects slip, i.e. the sliding at the contact boundary [3]. However, these methods often require the object to already be moving before any corrective signal is generated, and the reactive window may be too narrow to avoid a catastrophic fall.

The safer alternative is to infer friction during the initial press, before any tangential load is applied (Fig. 1A). This pre-lift estimation is precisely what humans do: grip force adjustments begin within 100 ms of contact, suggesting friction is perceived from normal press alone [4]. Previous work has linked this to the radial expansion of the fingertip skin, which is resisted by friction [5]. Friction modulates spatial shear at first contact, that can be decoded if the sensor has a sufficient spatial resolution.

Robotic implementations of pre-lift friction sensing have explored embedded sensing elements [6] and angled protrusions [7], but remain limited to flat surfaces. Here, we extend this capability to arbitrary geometries using a dense optical tactile sensor and a learned compact representation.

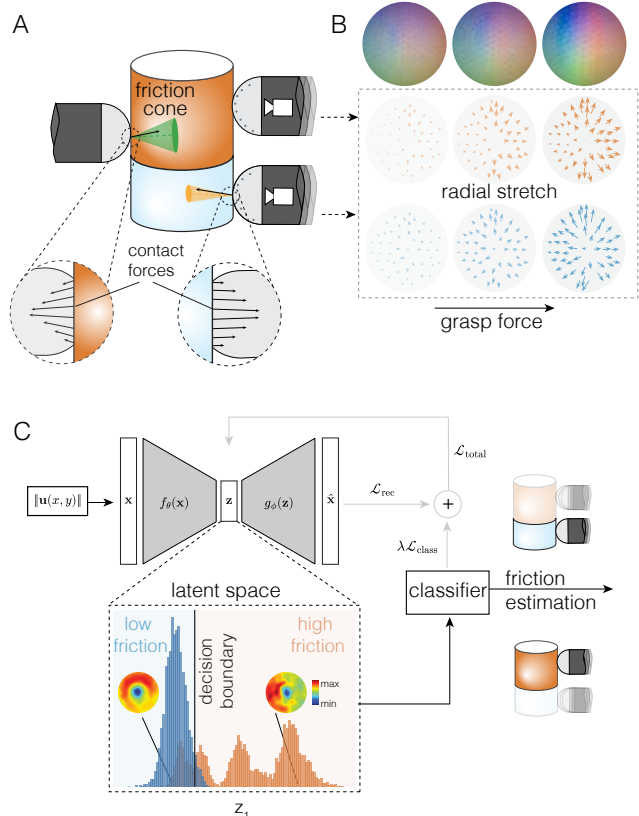


Fig. 1. **A.** Illustration of multiple sensors pressed against an object under two color-coded friction conditions. **B.** Images obtained with the ShadowTac sensor (top row). Lateral displacement associated with the two friction conditions. **C.** Model schematic: the  $\ell_2$ -normalized lateral displacement magnitude map is encoded into a single latent coordinate used for friction classification. Representative latent values are decoded into reconstructed deformation maps, illustrating the friction-dependent patterns learned by the model. The loss terms used during training are shown in light gray.

## METHODS

### A. Sensor and data acquisition

Tactile data were acquired with the ShadowTac sensor [8], tracking 180 surface markers embedded in a soft silicone membrane via a miniature camera. Each frame captured at 100 Hz results in a 2D lateral displacement field. From this field we computed the displacement magnitude map, a scalar image encoding the spatial distribution of shear intensity (Fig 1B).

A motorized stage pressed seven indenters (two spheres and two cylinders of 20 and 40 mm diameter, a flat surface, and two tilted flat surfaces oriented at 2.5° and 5°) against the tactile sensor at 1 mm/s. Indentation depth ranged from approximately 2-3 mm, depending on the geometry. Each geometry was tested under dry ( $\mu \approx 1.8 - 2.0$ ) and lubricated ( $\mu \approx 0.05 - 0.1$ ) conditions, repeated twice. Normal forces ranged from 2 to 7 N. Data were augmented by six rotations at 60° intervals with random jitter, resulting in 10,920 balanced samples. To encourage generalization across different force levels, training and validation sets were split by force: the model was trained on higher normal forces ( $F_n \in [5, 7]$  N), where frictional cues are more pronounced, and validated on lower forces ( $F_n \in [2, 5]$  N), where such cues are weaker.

### B. Model for friction estimation

A supervised autoencoder (SAE) was trained to simultaneously reconstruct the normalized input map and classify friction in the latent space. The training loss function was defined as the following  $L_{\text{total}} = L_{\text{rec}} + \lambda L_{\text{class}}$ , where  $L_{\text{rec}}$  and  $L_{\text{class}}$  are the losses associated with reconstruction and classification respectively, and  $\lambda$  is a classification weight. A linear classifier in the latent space was used to encourage separable clusters. Hyperparameters were selected based on validation accuracy: one latent dimension was sufficient to estimate friction, while additional dimensions provided only modest improvement. For the selected latent dimension  $d_z = 1$ , the best performing configuration used an encoder width of 256, a weight  $\lambda = 0.3$ , and a learning rate of  $10^{-3}$ .

## I. RESULTS

### A. Latent structure

Projecting the validation set onto  $z_1$  reveals two clusters corresponding to friction regimes dry and slippery, divided by a linear decision boundary (Fig 1C). Distributions grouped by geometry largely overlap, confirming that the model discards shape-specific information to retain only the friction-dependent structure of the shear deformation. One latent coordinate suffices for validation accuracy of 0.896 across all geometries and force ranges.

Classification accuracy increases with normal force, since higher load produces larger deformations. For most geometries, accuracy was already near perfect in the lowest force bin, suggesting that the corresponding deformation patterns were sufficiently discriminative at approximately 2 N (Fig 2A). The clearest force-dependent improvement was observed for the 40-mm spherical indenter, whose accuracy increased from approximately 65% in the 2-2.5 N bin to above 90% from the 4-4.5 N bin onward. The flat indenter remained poorly classified across the full force range, indicating that larger normal loads did not resolve the ambiguity observed in its latent distribution.

### B. Real-life experiments

To test the generalization of the method, the sensor was mounted on a robotic gripper and tested on seven previously

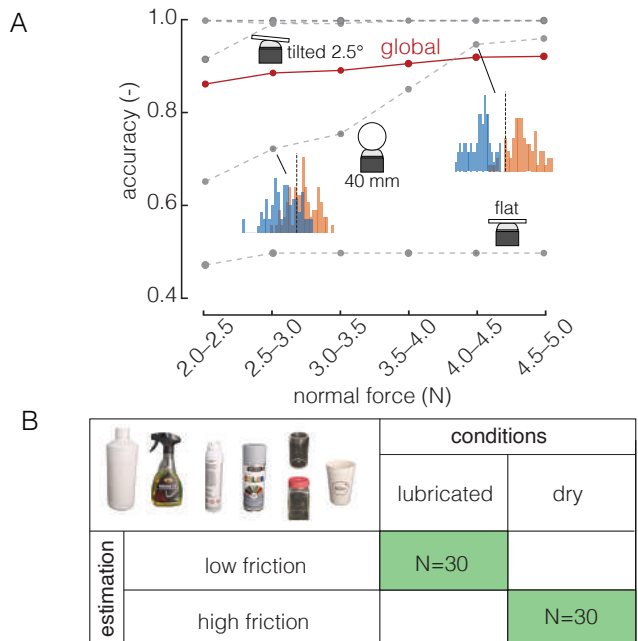


Fig. 2. **A**. Model accuracy across normal-force bins. Gray curves show individual geometries, the red curve shows aggregate accuracy, and insets show the increasing  $z_1$  separation for the 40-mm spherical indenter. **B**. Confusion matrix showing friction classification for 7 objects shown on the top left.

unseen objects (glass, plastic, metal; flat and curved surfaces) under dry and lubricated conditions (5 grasps each). The gripper was current-controlled to reach 4.5 N, then the grip force was ramped to 10 N and held for 300 ms. A contact was classified as slippery if more than 10 consecutive frames exceeded the linear decision boundary. The model correctly identified 100% of slippery contacts before any lift was attempted (Fig 2B).

## II. CONCLUSION AND DISCUSSION

We have demonstrated that a single normal press encodes sufficient information to classify surface friction with 89.6% of accuracy across diverse contact geometries using a one-dimensional latent representation. Friction modulates how lateral strain redistributes during compression: lubricated contacts produce symmetric, high-magnitude rings; dry contacts produce lower-magnitude, asymmetric fields caused by local membrane anchoring. These patterns are mechanically amplified by curvature and small contact eccentricities.

The approach extends prior pre-lift friction sensing from flat surfaces [9] to arbitrary geometries without specialized mechanical structures. The selected one-dimensional SAE trains in under a minute and requires only that the sensor provides spatially resolved shear maps, making it portable across optical tactile platforms.

Current limitations include binary friction classification (dry vs. lubricated) and the requirement for 10 N loading with the current membrane stiffness. A softer membrane would lower the detection threshold, broadening applicability to delicate

objects. Future work will target multi-level friction regression and integration with closed-loop grip force control after lift.

To our knowledge, this is the first geometry-invariant pre-lift friction estimation method using spatial shear alone, establishing friction as a mechanically observable quantity at the first instant of contact.

#### REFERENCES

- [1] A. Bicchi, "On the closure properties of robotic grasping," *The International Journal of Robotics Research*, vol. 14, no. 4, pp. 319–334, 1995.
- [2] M. T. Mason, *Mechanics of robotic manipulation*. MIT press, 2001.
- [3] W. Chen, H. Khamis, I. Birznieks, N. F. Lepora, and S. J. Redmond, "Tactile sensors for friction estimation and incipient slip detection—toward dexterous robotic manipulation: A review," *IEEE Sensors Journal*, vol. 18, no. 22, pp. 9049–9064, 2018.
- [4] R. S. Johansson and G. Westling, "Roles of glabrous skin receptors and sensorimotor memory in automatic control of precision grip when lifting rougher or more slippery objects," *Experimental brain research*, vol. 56, no. 3, pp. 550–564, 1984.
- [5] L. Willemet, K. Kanzari, J. Monnoyer, I. Birznieks, and M. Wiertelwski, "Initial contact shapes the perception of friction," *Proceedings of the National Academy of Sciences*, vol. 118, no. 49, p. e2109109118, 2021.
- [6] T. Okatani, H. Takahashi, K. Noda, T. Takahata, K. Matsumoto, and I. Shimoyama, "A tactile sensor using piezoresistive beams for detection of the coefficient of static friction," *Sensors*, vol. 16, no. 5, p. 718, 2016.
- [7] H. Khamis, B. Xia, and S. J. Redmond, "A novel optical 3d force and displacement sensor—towards instrumenting the papillarray tactile sensor," *Sensors and Actuators A: Physical*, vol. 291, pp. 174–187, 2019.
- [8] G. Vitrani, B. Pasquale, and M. Wiertelwski, "Shadowtac: Dense measurement of shear and normal deformation of a tactile membrane from colored shadows," in *2025 IEEE International Conference on Robotics and Automation (ICRA)*, pp. 5004–5010, IEEE, 2025.
- [9] T. Maeno, T. Kawamura, and S.-C. Cheng, "Friction estimation by pressing an elastic finger-shaped sensor against a surface," *IEEE Transactions on Robotics and Automation*, vol. 20, no. 2, pp. 222–228, 2004.